USC–SIPI REPORT #340

Energy Capture vs. Correlator Resources in Ultra-Wide Bandwidth Indoor Wireless Communications Channels

by

Moe Z. Win and Robert A. Scholtz

November 1997

Signal and Image Processing Institute
UNIVERSITY OF SOUTHERN CALIFORNIA
Department of Electrical Engineering-Systems
3740 McClintock Avenue, Room 400
Los Angeles, CA 90089-2564 U.S.A.

Energy Capture vs. Correlator Resources in Ultra-Wide Bandwidth Indoor Wireless Communications Channels

Moe Z. Win and Robert A. Scholtz
Communication Sciences Institute
Department of Electrical Engineering-Systems
University of Southern California, Los Angeles, CA 90089-2565 USA

Abstract—**The results of an ultra-wide bandwidth (UWB) signal propagation experiment performed in a typical modern office building are presented. The bandwidth of the signal used in this experiment is in excess of one GHz, which results in a multipath resolution of less than a nanosecond. The maximum likelihood (ML) detector, based on a specular multipath channel model, is derived to detect multipath components of measured waveforms. The results show that typical received waveforms consist of a finite number of dominant multipath components. The number of dominant multipath components is equivalent to the number of single-path signal correlators required in a UWB Rake receiver. The number of single-path signal correlators required to construct a filter matched to the received waveform, so that the constructed waveform adequately captures the average received signal energy, is a useful parameter for UWB Rake receiver design. The quantity *energy capture* is defined mathematically for use as a performance measure of the ML detector. Energy capture as a function of the number of single-path signal correlators is evaluated for each of the experimentally measured received waveforms, and typical results are presented.**

I. Introduction

THE EXISTENCE of multiple propagation paths (multipath) with different time delays gives rise to a complex time varying transmission channel and places fundamental limitations on the performance of wireless communications systems.

Many propagation measurements have been made over the years on both indoor and outdoor channels with much "narrower bandwidths" [1]–[18]. A comprehensive reference on the indoor propagation channels (a total of 281 references) can be found in the tutorial survey paper by Hashemi [9]. Some of the work by Rappaport [1]–[5] and a few other papers [6]–[8] are listed here as selected references. Although the research described in this paper does not cover outdoor propagation channels, the classic works on outdoor propagation channels by Turin [10], [11], by Cox [14]–[17], and by Nielson [18] are noted here for their excellent measurement procedures and data reduction techniques. However, these measurements are inadequate and characterization of ultra-wide bandwidth (UWB) signal propagation channels has not been available previously in the literature. Careful characterization of the UWB propagation channel is required to move beyond current limits and to determine methods for achieving fade resistant, mobile, high quality, robust communications.

The research described in this paper was supported in part by the Joint Services Electronics Program under contract F49620-94-0022, and in part by the Integrated Media Systems Center, a National Science Foundation Engineering Research Center with additional support from the Annenberg Center for Communication at the University of Southern California and the California Trade and Commerce Agency.

The authors can be reached by E-mail at win@milly.usc.edu, and scholtz@milly.usc.edu

II. Review of the UWB Propagation Experiment

An UWB signal propagation experiment was performed in a typical modern office building to characterize the UWB signal propagation channel [19]. The bandwidth of the signal used in this experiment was in excess of one GHz which results in a differential path delay resolution of less than a nanosecond. Extensive UWB signal propagation measurements were made in 14 different rooms and hallways on one floor of the modern office building using a periodic pulse generator that transmits pulses every 500 nanoseconds. In each office, multipath measurements over a 300 nanosecond wide window were made at 49 different locations. They are arranged spatially in a level 7x7 square grid with 6 inch spacing covering 3 feet by 3 feet. The same absolute delay reference for all recorded multipath profiles was achieved, and time delay measurements of the signals arriving at the receiving antenna via different propagation paths were made.

Figure 1 shows the transmitted pulses measured by the receiving antenna, located 1 m away from the transmitting antenna at the same height. Measurements were made while the vertically polarized receiving antenna was rotated about its axis in 45° steps. Measurements shown in Fig. 1 are labeled 0°, 45°, and 90°, where 0° refers to the case in which the transmitting and receiving antennas are facing each other. Figure 1 illustrates that the radiation pattern of the antenna used in the experiment is circularly symmetric around the vertical axis. The first 10 nanoseconds of the recorded waveforms in Fig. 1 represent a clean pulse arriving via the direct line of sight (LOS) path and not

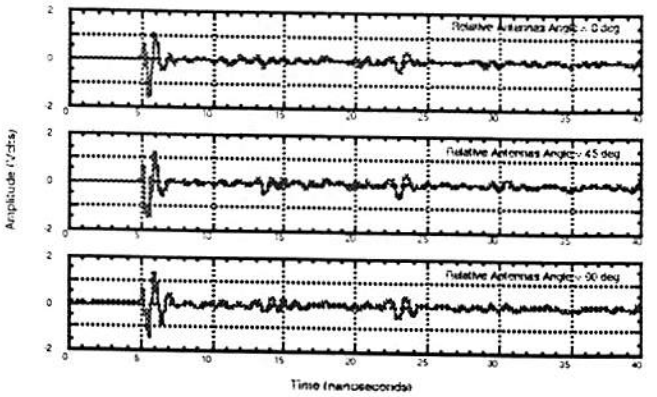

Fig. 1. Transmitted pulses measured by the receiving antenna located 1 m away from the transmitting antenna with the same height. Measurements were made while the vertically polarized receiving antenna is rotated about its axis, where 0° refers to the case in which the transmitting and the receiving antenna are facing at each other.

corrupted by multipath components.

Figure 2 shows the typical multipath profiles measured along a horizontal line of the grid at three different positions one foot apart. This represents typical UWB signal transmissions for a "high SNR" environment. Notice that the direct path response (leading edge of the responses) suggests that the location of the receiver for the lower trace is closer to the transmitter than that of the upper trace. Similar results are given in Fig. 3 representing typical UWB signal transmissions for a "low SNR" environment. Note that the first arriving path is not always the strongest path. Multipath delay spreads on the order of a hundred nanoseconds were observed.[1]

III. Multipath Channel

A. Multipath Channel Model

In general, multipath channels (especially indoor channels) consist of many path components. However, only a finite number of dominant multipath components exist in a typical received waveform. It is desirable to find the L_p most dominant paths, where the number L_p is proportional to the receiver's complexity in the communication system design. In the existing literature, this is typically accomplished by discretizing the delay axis into bins of $\Delta\tau$ seconds. If the integrated power within the i^{th} delay bin interval c_i^2 of the received signal $r(t)$ exceeds the chosen minimum detectable signal threshold, a multipath component with magnitude $|c_i|$ is said to exist at delay $\tau_i = i\Delta\tau$. The L_p paths corresponding to the largest values of $|c_i|$ may then be chosen as the dominant paths [3], [4]. The number of multipath components also influences the choice of channel modeling techniques. If the number of multipath components is small (≈ 5), then they can be attributed to the obvious reflecting objects in the channel and a ray tracing model, based on the building geometry, is a plausible choice. On the other hand, ray tracing techniques become site specific and their computational complexity becomes a burden when the number of multipath components is large [4].

From the view point of Rake receiver design, it is desired to model the received signal $r(t)$ by a linear combinations of a basic waveform $w(t)$ and its delay versions. Specifically,

[1] Measured waveforms in a 300 nanosecond wide window are not shown in this paper in attempt to reduce the paper length. Detailed results of the UWB signal propagation experiment can be found in [19]

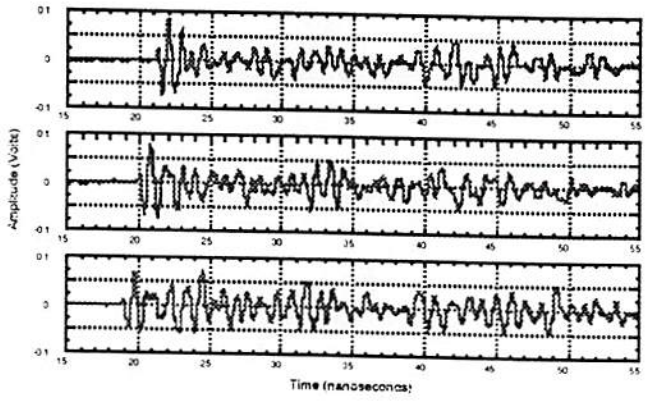

Fig. 2. Averaged multipath profiles in a 40 nanosecond window measured in an office, along a horizontal line of the grid at three different positions one foot apart. The transmitter is approximately 6 meters from the receiver, representing typical UWB signal transmission for the "high SNR" environment.

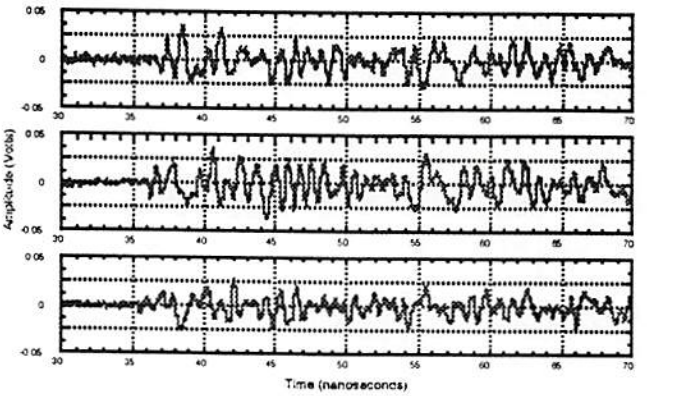

Fig. 3. Averaged multipath profiles in a 40 nanosecond window measured in an office, along a horizontal line of the grid at three different positions one foot apart. The transmitter is approximately 10 meters from the receiver, representing typical UWB signal transmission for the "low SNR" environment.

the received signal model is given by

$$r(t) \approx \sum_{i=1}^{L_p} c_i w(t-\tau_i) + n(t). \quad (1)$$

The observation noise $n(t)$ is modeled as additive white Gaussian noise (AWGN). It is important to stress that the parameters c_i and τ_i are modeled as *continuous* random variables representing the amplitude and the delay (in time) of the i^{th} multipath component. The waveform $w(t)$ can be viewed as a template waveform built into the receiver for use in Rake correlator structures [20], [21]. A typical shape of the waveform $w(t)$ is shown in Fig. 4, and it is assumed that $w(t)$ is reasonably similar to the isolated path signals in the whole ensemble of measured received waveforms. The simple specular model given by (1) is a natural choice for a resolvable UWB multipath channel.

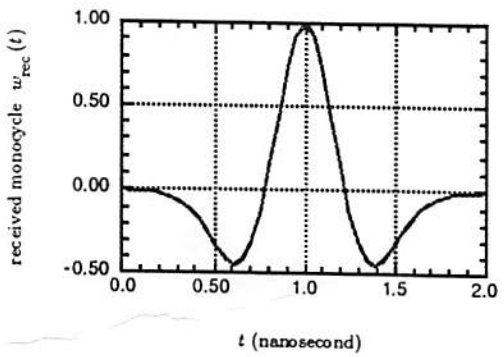

Fig. 4. A typical idealized waveform as a function of time in nanoseconds. The model used in this plot is $w_{rec}(t+1.0) = [1 - 4\pi(t/\tau_m)^2]\exp[-2\pi(t/\tau_m)^2]$ with $\tau_m = 0.78125$, which is assumed to be reasonably well-matched to the isolated paths in the whole ensemble of measured received waveforms.

B. The Optimal Multipath Detector

Given a specific received signal $r(t)$ over an observation interval $[0,T)$, and for a given number of dominant multipath components L_p, the goal is to find the "best" values of $\{\hat{c}_i\}_{i=1}^{L_p}$ and $\{\hat{\tau}_i\}_{i=1}^{L_p}$, such that the synthesized waveform $\sum_{i=1}^{L_p} \hat{c}_i w(t-\hat{\tau}_i)$ is well matched to the received waveform $r(t)$. In this paper, the optimal maximum likelihood (ML) detector is derived. Since $n(t)$ is modeled as AWGN, the ML detector is equivalent to a minimum mean squared error detector, i.e., the maximum likelihood estimates of $\hat{c}_i$ and $\hat{\tau}_i$ are the values of c_i and τ_i such that $\int_0^T |r(t) - \sum_{i=1}^{L_p} c_i w(t-\tau_i)|^2 dt$ is minimized. For a given L_p, let $\mathbf{c}$ and $\boldsymbol{\tau}$ be the amplitude and the delay vectors, with dimension $L_p \times 1$, defined by

$$\mathbf{c} \triangleq \begin{bmatrix} c_1 \\ c_2 \\ \vdots \\ c_{L_p} \end{bmatrix}, \quad \text{and} \quad \boldsymbol{\tau} \triangleq \begin{bmatrix} \tau_1 \\ \tau_2 \\ \vdots \\ \tau_{L_p} \end{bmatrix}. \quad (2)$$

The maximum likelihood estimates of the delay vector $\hat{\boldsymbol{\tau}}$ and amplitude vector $\hat{\mathbf{c}}$ were derived in [22], and it was shown to result in decoupled solutions as

$$\hat{\boldsymbol{\tau}} = \underset{\boldsymbol{\tau}}{\text{argmax}} \{\boldsymbol{\chi}^\dagger(\boldsymbol{\tau}) \mathbf{R}^{-1} \boldsymbol{\chi}(\boldsymbol{\tau})\} \quad (3)$$

$$\hat{\mathbf{c}} = \mathbf{R}^{-1} \boldsymbol{\chi}(\hat{\boldsymbol{\tau}}). \quad (4)$$

The vector $\boldsymbol{\chi}(\boldsymbol{\tau})$ is given by

$$\boldsymbol{\chi}(\boldsymbol{\tau}) = \int_0^T r(t) \begin{bmatrix} w(t-\tau_1) \\ w(t-\tau_2) \\ \vdots \\ w(t-\tau_{L_p}) \end{bmatrix} dt, \quad (5)$$

where the components of $\boldsymbol{\chi}(\boldsymbol{\tau})$ can be interpreted as the correlation of the received signal $r(t)$ with $w(t)$ at different hypothesized delays. The correlation matrix $\mathbf{R}$ is given by

$$\mathbf{R} = \begin{bmatrix} R(\tau_1-\tau_1) & R(\tau_1-\tau_2) & \dots & R(\tau_1-\tau_{L_p}) \\ R(\tau_2-\tau_1) & R(\tau_2-\tau_2) & \dots & R(\tau_2-\tau_{L_p}) \\ \dots & \dots & \dots & \dots \\ R(\tau_{L_p}-\tau_1) & R(\tau_{L_p}-\tau_2) & \dots & R(\tau_{L_p}-\tau_{L_p}) \end{bmatrix}$$

where

$$R(\tau_i - \tau_j) = \int_0^T w(t-\tau_i)\, w(t-\tau_j) dt. \quad (6)$$

For wide bandwidth transmission channel modeling, it is often assumed that the multipath channel is separable, i.e.,

$$|\tau_i - \tau_j| > \text{width of } w(t) \quad \text{for all} \quad i \neq j. \quad (7)$$

This approximation is even more valid in the case of UWB transmission channel. Under this assumption $R(\tau_i - \tau_j) = 0$ for all $i \neq j$, and

$$\mathbf{R} = \begin{bmatrix} R(0) & 0 & \dots & 0 \\ 0 & R(0) & \dots & 0 \\ \dots & \dots & \dots & \dots \\ 0 & 0 & \dots & R(0) \end{bmatrix}. \quad (8)$$

Simple matrix manipulation shows that

$$\boldsymbol{\chi}^\dagger(\boldsymbol{\tau}) \mathbf{R}^{-1} \boldsymbol{\chi}(\boldsymbol{\tau}) = \sum_{i=1}^{L_p} \frac{1}{R(0)} |\chi(\tau_i)|^2, \quad (9)$$

where

$$\chi(\tau_i) = \int_0^T r(t) w(t-\tau_i) dt. \quad (10)$$

Therefore, the maximum likelihood estimates of the delay vector $\hat{\boldsymbol{\tau}}$ and amplitude vector $\hat{\mathbf{c}}$ for a separable multipath channel become

$$\hat{\boldsymbol{\tau}} = \underset{\boldsymbol{\tau}}{\text{argmax}} \left\{ \sum_{i=1}^{L_p} \left| \frac{\chi(\tau_i)}{\sqrt{R(0)}} \right| \right\} \quad (11)$$

$$\hat{\mathbf{c}} = \frac{\boldsymbol{\chi}(\hat{\boldsymbol{\tau}})}{R(0)}. \quad (12)$$

IV. Performance Measure and Results

The performance measure of the multipath detector will be made in terms of the quantity *energy capture*. Energy capture as a function of L_p is defined mathematically as

$$EC(L_p) = \left\{ 1 - \underbrace{\frac{||r(t) - \sum_{i=1}^{L_p} \hat{c}_i w(t - \hat{\tau}_i)||^2}{||r(t)||^2}}_{\triangleq \text{ normalized MSE}} \right\} \times 100\%. \quad (13)$$

The number L_p can be interpreted as the number of single-path signal correlators required in a UWB Rake receiver to construct a filter matched to the received waveform, so that the constructed waveform "adequately" captures the average received signal energy.

Energy capture as a function of the number of correlators is computed for each received waveform measurement. The number of required single-path signal correlators in a UWB Rake receiver versus percentage energy capture is plotted in Fig. 5 for 49 received waveforms in an office representing a typical "high SNR" environment. Similar results for a typical "low SNR" environment are given in Fig. 6. Note that the amount of capture energy increase rapidly as the number of single-path signal correlators increases from 0 to 50. However, this improvement becomes gradual as the number of single-path signal correlators increases from 50 to 100. Beyond this point, only negligible improvement can be made as the number of single-path signal correlators increases. In practice, UWB Rake receivers are designed to operate in regions where the increase in energy capture as a function of the number of single-path signal correlators is rapid. Figures 5 and 6 also suggest that the number of dominant specular multipath components is expected to be less than 50 for UWB signal transmissions in a typical modern office building. On the other hand, the number of dominant specular multipath components is much larger than 5.

V. Conclusions and Caveats

Multipath components of experimentally measured received waveforms are detected using the ML detector which is derived based on a specular multipath channel model. Energy capture as a function of the number of single-path signal correlators used in a UWB Rake receiver is evaluated for each of the experimentally measured received waveforms. The amount of energy capture increases rapidly as the the number of single-path signal correlators increases from 0 to 50. However, this improvement becomes gradual and only negligible improvement can be made as the number of single-path signal correlators increases beyond 100. The results show that the number of dominant specular multipath components is less than 50 for UWB signal transmissions in a typical modern office building. On the other hand, the number of dominant specular multipath components is much larger than 5, which suggests that ray tracing techniques may not be feasible for modeling UWB indoor wireless communications channels in typical modern office buildings.

The results presented in this paper are based on the simple specular model given by (1). However, it seems plausible that later multipath components may incur more distortion than earlier arriving multipath components. This suggests the use of a family of basic waveforms $\{w^l(t)\}_{l=1}^N$ and determination of the "best" choice of $\left\{ \{\hat{c}_i^l\}_{i=1}^{L_p}, \{\hat{\tau}_i^l\}_{i=1}^{L_p} \right\}_{l=1}^N$ such that the synthesized waveform $\sum_{l=1}^N \sum_{i=1}^{L_p} \hat{c}_i^l w^l(t - \hat{\tau}_i^l)$ is well matched to the received waveform $r(t)$.

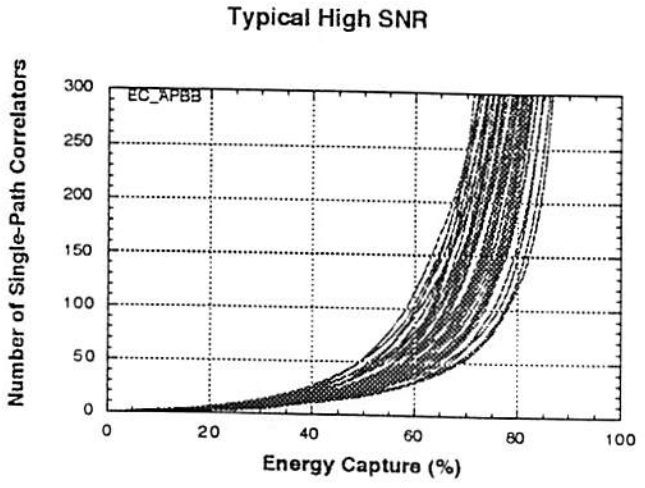

Fig. 5. The number of single-path signal correlators in a UWB Rake receiver as a function of percentage energy capture for each of the 49 received waveforms in an office representing typical "high SNR" environment.

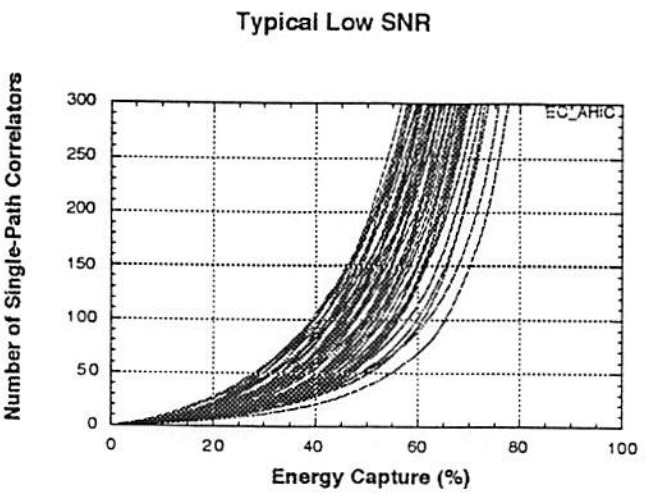

Fig. 6. The number of single-path signal correlators in a UWB Rake receiver as a function of percentage energy capture for each of the 49 received waveforms in an office representing typical "low SNR" environment.

ACKNOWLEDGMENTS

The authors wish to thank Mark A. Barnes, Alan Petroff and Larry Fullerton of Time Domain Systems, and Paul Withington of Pulson Communications for several helpful discussions concerning the technology, capabilities, and signal processing of impulse signals.

REFERENCES

[1] J. B. Andersen, T. S. Rappaport, and S. Yoshida, "Propagation measurements and models for wireless communications channels," *IEEE Commun. Mag.*, vol. 33, pp. 42–49, Jan. 1995.

[2] T. S. Rappaport and C. D. McGillem, "UHF fading in factories," *IEEE J. Select. Areas Commun.*, vol. SAC-7, pp. 40–48, Jan. 1989.

[3] T. S. Rappaport, "Characterization of UHF multipath radio channels in factory buildings," *IEEE Trans. Antennas Propagat.*, vol. AP-37, pp. 1058–1069, Aug. 1989.

[4] T. S. Rappaport, S. Y. Seidel, and K. Takamizawa, "Statistical channel impulse response models for factory an open plan building radio communication system design," *IEEE Trans. Commun.*, vol. COM-39, pp. 794–807, May 1991.

[5] S. Y. Seidel and T. S. Rappaport, "914 MHz path loss prediction models for indoor wireless communications in multifloored buildings," *IEEE Trans. Antennas Propagat.*, vol. AP-40, pp. 207–217, Feb. 1992.

[6] D. M. J. Devasirvatham, "Multipath time delay jitter measured at 850 MHz in the portable radio environment," *IEEE J. Select. Areas Commun.*, vol. SAC-5, pp. 855–861, June 1987.

[7] A. A. Saleh and R. A. Valenzuela, "A statistical model for indoor multipath propagation," *IEEE J. Select. Areas Commun.*, vol. SAC-5, pp. 128–137, Feb. 1987.

[8] R. J. Bultitude, S. A. Mahmoud, and W. A. Sullivan, "A comparison of indoor radio propagation characteristics at 910 MHz and 1.75 GHz," *IEEE J. Select. Areas Commun.*, vol. SAC-7, pp. 20–30, Jan. 1989.

[9] H. Hashemi, "The indoor radio propagation channel," *Proc. IEEE*, vol. 81, pp. 943–968, July 1993.

[10] G. Turin, F. D. Clapp, T. L. Johnston, S. B. Fine, and D. Lavry, "A statistical model of urban multipath propagation," *IEEE Trans. on Vehicul. Technol.*, vol. VT-21, pp. 1–9, Feb. 1972.

[11] G. Turin, "Introduction to spread-spectrum antimultipath techniques and their application to urban digital radio," *Proc. IEEE*, vol. 68, pp. 328–353, Mar. 1980.

[12] H. Suzuki, "A statistical model for urban radio propagation," *IEEE Trans. Commun.*, vol. 25, pp. 673–680, July 1977.

[13] H. Hashemi, "Simulation of the urban radio propagation channel," *IEEE Trans. on Vehicul. Technol.*, vol. VT-28, pp. 213–225, Aug. 1979.

[14] D. C. Cox, "Delay doppler characteristics of multipath propagation at 910 MHz in a suburban mobile radio environment," *IEEE Trans. Antennas Propagat.*, vol. AP-20, pp. 625–635, Sept. 1972.

[15] D. C. Cox, "Time- and frequency-domain characterizations of multipath propagation at 910 MHz in a suburban mobile-radio environment," *Radio Science*, pp. 1069–1077, Dec. 1972.

[16] D. C. Cox, "910 MHz urban mobile radio propagation: Multipath characteristics in New York city," *IEEE Trans. Commun.*, vol. COM-21, pp. 1188–1194, Nov. 1973.

[17] D. C. Cox and R. P. Leck, "Distributions of multipath delay spread and average excess delay for 910-MHz urban mobile radio paths," *IEEE Trans. Antennas Propagat.*, vol. AP-23, pp. 206–213, Mar. 1975.

[18] D. L. Nielson, "Microwave propagation measurements for mobile digital radio application," *IEEE Trans. on Vehicul. Technol.*, vol. VT-28, pp. 117–132, Aug. 1978.

[19] M. Z. Win, R. A. Scholtz, and M. A. Barnes, "Ultra-wide bandwidth signal propagation for indoor wireless communications," in *Proc. IEEE Int. Conf. on Comm.*, pp. 56–60, June 1997. Montréal, Canada.

[20] R. Price and P. E. Green, Jr., "A communication technique for multipath channels," *Proc. IRE*, vol. 46, pp. 555–570, Mar. 1958.

[21] J. G. Proakis, *Digital Communications*. McGraw-Hill, Inc., third ed., 1995.

[22] M. Z. Win and R. A. Scholtz, "Characterization of ultra-wide bandwidth wireless indoor communications channel: A communications theoretic view," *IEEE Trans. Commun.*, Nov. 1997. submitted.

Energy Capture vs. Correlator Resources in Ultra-Wide Bandwidth Indoor Wireless Communications Channels

Moe Z. Win and Robert A. Scholtz
Communication Sciences Institute
Department of Electrical Engineering-Systems
University of Southern California, Los Angeles, CA 90089-2565 USA

Abstract—**The results of an ultra-wide bandwidth (UWB) signal propagation experiment performed in a typical modern office building are presented. The bandwidth of the signal used in this experiment is in excess of one GHz, which results in a multipath resolution of less than a nanosecond. The maximum likelihood (ML) detector, based on a specular multipath channel model, is derived to detect multipath components of measured waveforms. The results show that typical received waveforms consist of a finite number of dominant multipath components. The number of dominant multipath components is equivalent to the number of single-path signal correlators required in a UWB Rake receiver. The number of single-path signal correlators required to construct a filter matched to the received waveform, so that the constructed waveform adequately captures the average received signal energy, is a useful parameter for UWB Rake receiver design. The quantity *energy capture* is defined mathematically for use as a performance measure of the ML detector. Energy capture as a function of the number of single-path signal correlators is evaluated for each of the experimentally measured received waveforms, and typical results are presented.**

I. Introduction

THE EXISTENCE of multiple propagation paths (multipath) with different time delays gives rise to a complex time varying transmission channel and places fundamental limitations on the performance of wireless communications systems.

Many propagation measurements have been made over the years on both indoor and outdoor channels with much "narrower bandwidths" [1]–[18]. A comprehensive reference on the indoor propagation channels (a total of 281 references) can be found in the tutorial survey paper by Hashemi [9]. Some of the work by Rappaport [1]–[5] and a few other papers [6]–[8] are listed here as selected references. Although the research described in this paper does not cover outdoor propagation channels, the classic works on outdoor propagation channels by Turin [10], [11], by Cox [14]–[17], and by Nielson [18] are noted here for their excellent measurement procedures and data reduction techniques. However, these measurements are inadequate and characterization of ultra-wide bandwidth (UWB) signal propagation channels has not been available previously in the literature. Careful characterization of the UWB propagation channel is required to move beyond current limits and to determine methods for achieving fade resistant, mobile, high quality, robust communications.

The research described in this paper was supported in part by the Joint Services Electronics Program under contract F49620-94-0022, and in part by the Integrated Media Systems Center, a National Science Foundation Engineering Research Center with additional support from the Annenberg Center for Communication at the University of Southern California and the California Trade and Commerce Agency.

The authors can be reached by E-mail at win@milly.usc.edu, and scholtz@milly.usc.edu

II. Review of the UWB Propagation Experiment

An UWB signal propagation experiment was performed in a typical modern office building to characterize the UWB signal propagation channel [19]. The bandwidth of the signal used in this experiment was in excess of one GHz which results in a differential path delay resolution of less than a nanosecond. Extensive UWB signal propagation measurements were made in 14 different rooms and hallways on one floor of the modern office building using a periodic pulse generator that transmits pulses every 500 nanoseconds. In each office, multipath measurements over a 300 nanosecond wide window were made at 49 different locations. They are arranged spatially in a level 7x7 square grid with 6 inch spacing covering 3 feet by 3 feet. The same absolute delay reference for all recorded multipath profiles was achieved, and time delay measurements of the signals arriving at the receiving antenna via different propagation paths were made.

Figure 1 shows the transmitted pulses measured by the receiving antenna, located 1 m away from the transmitting antenna at the same height. Measurements were made while the vertically polarized receiving antenna was rotated about its axis in 45° steps. Measurements shown in Fig. 1 are labeled 0°, 45°, and 90°, where 0° refers to the case in which the transmitting and receiving antennas are facing each other. Figure 1 illustrates that the radiation pattern of the antenna used in the experiment is circularly symmetric around the vertical axis. The first 10 nanoseconds of the recorded waveforms in Fig. 1 represent a clean pulse arriving via the direct line of sight (LOS) path and not

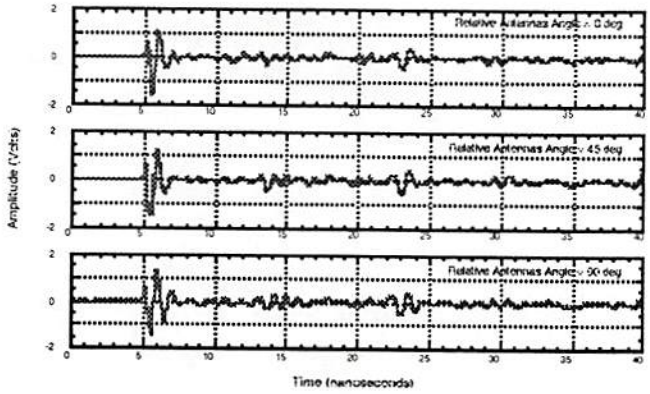

Fig. 1. Transmitted pulses measured by the receiving antenna located 1 m away from the transmitting antenna with the same height. Measurements were made while the vertically polarized receiving antenna is rotated about its axis, where 0° refers to the case in which the transmitting and the receiving antenna are facing at each other.

corrupted by multipath components.

Figure 2 shows the typical multipath profiles measured along a horizontal line of the grid at three different positions one foot apart. This represents typical UWB signal transmissions for a "high SNR" environment. Notice that the direct path response (leading edge of the responses) suggests that the location of the receiver for the lower trace is closer to the transmitter than that of the upper trace. Similar results are given in Fig. 3 representing typical UWB signal transmissions for a "low SNR" environment. Note that the first arriving path is not always the strongest path. Multipath delay spreads on the order of a hundred nanoseconds were observed.[1]

III. Multipath Channel

A. Multipath Channel Model

In general, multipath channels (especially indoor channels) consist of many path components. However, only a finite number of dominant multipath components exist in a typical received waveform. It is desirable to find the L_p most dominant paths, where the number L_p is proportional to the receiver's complexity in the communication system design. In the existing literature, this is typically accomplished by discretizing the delay axis into bins of $\Delta\tau$ seconds. If the integrated power within the $i^{\underline{\text{th}}}$ delay bin interval c_i^2 of the received signal $r(t)$ exceeds the chosen minimum detectable signal threshold, a multipath component with magnitude $|c_i|$ is said to exist at delay $\tau_i = i\Delta\tau$. The L_p paths corresponding to the largest values of $|c_i|$ may then be chosen as the dominant paths [3], [4]. The number of multipath components also influences the choice of channel modeling techniques. If the number of multipath components is small (≈ 5), then they can be attributed to the obvious reflecting objects in the channel and a ray tracing model, based on the building geometry, is a plausible choice. On the other hand, ray tracing techniques become site specific and their computational complexity becomes a burden when the number of multipath components is large [4].

From the view point of Rake receiver design, it is desired to model the received signal $r(t)$ by a linear combinations of a basic waveform $w(t)$ and its delay versions. Specifically,

[1]Measured waveforms in a 300 nanosecond wide window are not shown in this paper in attempt to reduce the paper length. Detailed results of the UWB signal propagation experiment can be found in [19]

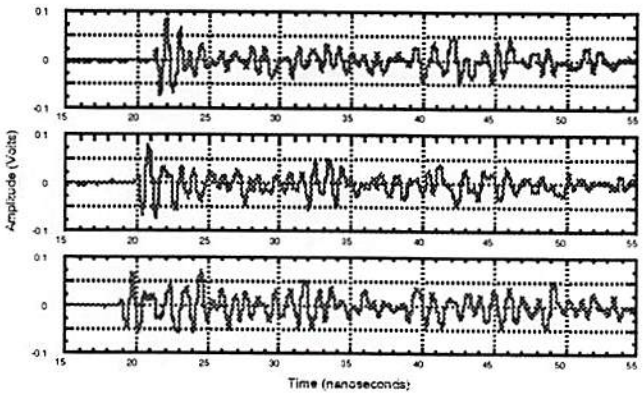

Fig. 2. Averaged multipath profiles in a 40 nanosecond window measured in an office, along a horizontal line of the grid at three different positions one foot apart. The transmitter is approximately 6 meters from the receiver, representing typical UWB signal transmission for the "high SNR" environment.

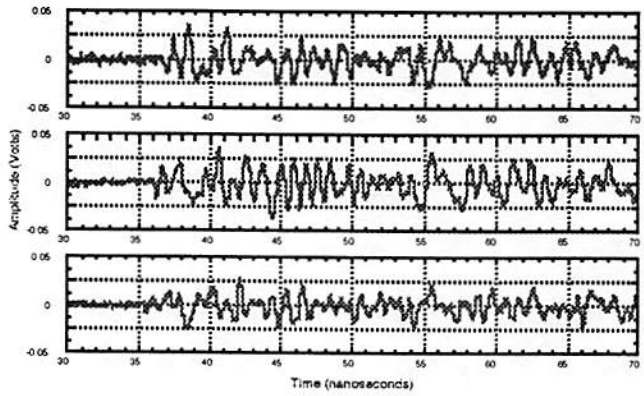

Fig. 3. Averaged multipath profiles in a 40 nanosecond window measured in an office, along a horizontal line of the grid at three different positions one foot apart. The transmitter is approximately 10 meters from the receiver, representing typical UWB signal transmission for the "low SNR" environment.

the received signal model is given by

$$r(t) \approx \sum_{i=1}^{L_p} c_i w(t-\tau_i) + n(t)\,. \tag{1}$$

The observation noise $n(t)$ is modeled as additive white Gaussian noise (AWGN). It is important to stress that the parameters c_i and τ_i are modeled as *continuous* random variables representing the amplitude and the delay (in time) of the i^{th} multipath component. The waveform $w(t)$ can be viewed as a template waveform built into the receiver for use in Rake correlator structures [20], [21]. A typical shape of the waveform $w(t)$ is shown in Fig. 4, and it is assumed that $w(t)$ is reasonably similar to the isolated path signals in the whole ensemble of measured received waveforms. The simple specular model given by (1) is a natural choice for a resolvable UWB multipath channel.

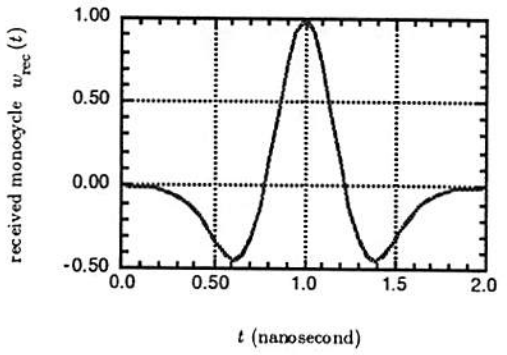

Fig. 4. A typical idealized waveform as a function of time in nanoseconds. The model used in this plot is $w_{\text{rec}}(t+1.0) = [1 - 4\pi(t/\tau_{\text{m}})^2]\exp[-2\pi(t/\tau_{\text{m}})^2]$ with $\tau_{\text{m}} = 0.78125$, which is assumed to be reasonably well-matched to the isolated paths in the whole ensemble of measured received waveforms.

B. The Optimal Multipath Detector

Given a specific received signal $r(t)$ over an observation interval $[0,T)$, and for a given number of dominant multipath components L_{p}, the goal is to find the "best" values of $\{\hat{c}_i\}_{i=1}^{L_{\text{p}}}$ and $\{\hat{\tau}_i\}_{i=1}^{L_{\text{p}}}$, such that the synthesized waveform $\sum_{i=1}^{L_{\text{p}}} \hat{c}_i w(t-\hat{\tau}_i)$ is well matched to the received waveform $r(t)$. In this paper, the optimal maximum likelihood (ML) detector is derived. Since $n(t)$ is modeled as AWGN, the ML detector is equivalent to a minimum mean squared error detector, i.e., the maximum likelihood estimates of $\hat{c}_i$ and $\hat{\tau}_i$ are the values of c_i and τ_i such that $\int_0^T |r(t) - \sum_{i=1}^{L_{\text{p}}} c_i w(t-\tau_i)|^2 dt$ is minimized. For a given L_{p}, let $\mathbf{c}$ and $\boldsymbol{\tau}$ be the amplitude and the delay vectors, with dimension $L_{\text{p}} \times 1$, defined by

$$\mathbf{c} \triangleq \begin{bmatrix} c_1 \\ c_2 \\ \vdots \\ c_{L_{\text{p}}} \end{bmatrix}, \quad \text{and} \quad \boldsymbol{\tau} \triangleq \begin{bmatrix} \tau_1 \\ \tau_2 \\ \vdots \\ \tau_{L_{\text{p}}} \end{bmatrix}. \tag{2}$$

The maximum likelihood estimates of the delay vector $\hat{\boldsymbol{\tau}}$ and amplitude vector $\hat{\mathbf{c}}$ were derived in [22], and it was shown to result in decoupled solutions as

$$\hat{\boldsymbol{\tau}} = \underset{\boldsymbol{\tau}}{\text{argmax}}\{\boldsymbol{\chi}^{\dagger}(\boldsymbol{\tau})\mathbf{R}^{-1}\boldsymbol{\chi}(\boldsymbol{\tau})\} \tag{3}$$

$$\hat{\mathbf{c}} = \mathbf{R}^{-1}\boldsymbol{\chi}(\hat{\boldsymbol{\tau}})\,. \tag{4}$$

The vector $\boldsymbol{\chi}(\boldsymbol{\tau})$ is given by

$$\boldsymbol{\chi}(\boldsymbol{\tau}) = \int_0^T r(t) \begin{bmatrix} w(t-\tau_1) \\ w(t-\tau_2) \\ \vdots \\ w(t-\tau_{L_{\text{p}}}) \end{bmatrix} dt\,, \tag{5}$$

where the components of $\boldsymbol{\chi}(\boldsymbol{\tau})$ can be interpreted as the correlation of the received signal $r(t)$ with $w(t)$ at different hypothesized delays. The correlation matrix $\mathbf{R}$ is given by

$$\mathbf{R} = \begin{bmatrix} R(\tau_1-\tau_1) & R(\tau_1-\tau_2) & \dots & R(\tau_1-\tau_{L_{\text{p}}}) \\ R(\tau_2-\tau_1) & R(\tau_2-\tau_2) & \dots & R(\tau_2-\tau_{L_{\text{p}}}) \\ \dots & \dots & \dots & \dots \\ R(\tau_{L_{\text{p}}}-\tau_1) & R(\tau_{L_{\text{p}}}-\tau_2) & \dots & R(\tau_{L_{\text{p}}}-\tau_{L_{\text{p}}}) \end{bmatrix}$$

where

$$R(\tau_i - \tau_j) = \int_0^T w(t-\tau_i)\, w(t-\tau_j) dt\,. \tag{6}$$

For wide bandwidth transmission channel modeling, it is often assumed that the multipath channel is separable, i.e.,

$$|\tau_i - \tau_j| > \text{width of } w(t) \qquad \text{for all} \qquad i \neq j\,. \tag{7}$$

This approximation is even more valid in the case of UWB transmission channel. Under this assumption $R(\tau_i - \tau_j) = 0$ for all $i \neq j$, and

$$\mathbf{R} = \begin{bmatrix} R(0) & 0 & \dots & 0 \\ 0 & R(0) & \dots & 0 \\ \dots & \dots & \dots & \dots \\ 0 & 0 & \dots & R(0) \end{bmatrix}. \tag{8}$$

Simple matrix manipulation shows that

$$\boldsymbol{\chi}^{\dagger}(\boldsymbol{\tau})\mathbf{R}^{-1}\boldsymbol{\chi}(\boldsymbol{\tau}) = \sum_{i=1}^{L_{\text{p}}} \frac{1}{R(0)} |\chi(\tau_i)|^2\,, \tag{9}$$

where

$$\chi(\tau_i) = \int_0^T r(t) w(t-\tau_i) dt\,. \tag{10}$$

Therefore, the maximum likelihood estimates of the delay vector $\hat{\boldsymbol{\tau}}$ and amplitude vector $\hat{\mathbf{c}}$ for a separable multipath channel become

$$\hat{\boldsymbol{\tau}} = \underset{\boldsymbol{\tau}}{\text{argmax}} \left\{ \sum_{i=1}^{L_{\text{p}}} \left| \frac{\chi(\tau_i)}{\sqrt{R(0)}} \right| \right\} \tag{11}$$

$$\hat{\mathbf{c}} = \frac{\boldsymbol{\chi}(\hat{\boldsymbol{\tau}})}{R(0)}\,. \tag{12}$$

IV. Performance Measure and Results

The performance measure of the multipath detector will be made in terms of the quantity *energy capture*. Energy capture as a function of L_p is defined mathematically as

$$EC(L_p) = \left\{ 1 - \underbrace{\frac{||r(t) - \sum_{i=1}^{L_p} \hat{c}_i w(t - \hat{\tau}_i)||^2}{||r(t)||^2}}_{\triangleq \text{ normalized MSE}} \right\} \times 100\%. \quad (13)$$

The number L_p can be interpreted as the number of single-path signal correlators required in a UWB Rake receiver to construct a filter matched to the received waveform, so that the constructed waveform "adequately" captures the average received signal energy.

Energy capture as a function of the number of correlators is computed for each received waveform measurement. The number of required single-path signal correlators in a UWB Rake receiver versus percentage energy capture is plotted in Fig. 5 for 49 received waveforms in an office representing a typical "high SNR" environment. Similar results for a typical "low SNR" environment are given in Fig. 6. Note that the amount of capture energy increase rapidly as the number of single-path signal correlators increases from 0 to 50. However, this improvement becomes gradual as the number of single-path signal correlators increases from 50 to 100. Beyond this point, only negligible improvement can be made as the number of single-path signal correlators increases. In practice, UWB Rake receivers are designed to operate in regions where the increase in energy capture as a function of the number of single-path signal correlators is rapid. Figures 5 and 6 also suggest that the number of dominant specular multipath components is expected to be less than 50 for UWB signal transmissions in a typical modern office building. On the other hand, the number of dominant specular multipath components is much larger than 5.

V. Conclusions and Caveats

Multipath components of experimentally measured received waveforms are detected using the ML detector which is derived based on a specular multipath channel model. Energy capture as a function of the number of single-path signal correlators used in a UWB Rake receiver is evaluated for each of the experimentally measured received waveforms. The amount of energy capture increases rapidly as the the number of single-path signal correlators increases from 0 to 50. However, this improvement becomes gradual and only negligible improvement can be made as the number of single-path signal correlators increases beyond 100. The results show that the number of dominant specular multipath components is less than 50 for UWB signal transmissions in a typical modern office building. On the other hand, the number of dominant specular multipath components is much larger than 5, which suggests that ray tracing techniques may not be feasible for modeling UWB indoor wireless communications channels in typical modern office buildings.

The results presented in this paper are based on the simple specular model given by (1). However, it seems plausible that later multipath components may incur more distortion than earlier arriving multipath components. This suggests the use of a family of basic waveforms $\{w^l(t)\}_{l=1}^N$ and determination of the "best" choice of $\left\{ \{\hat{c}_i^l\}_{i=1}^{L_p}, \{\hat{\tau}_i^l\}_{i=1}^{L_p} \right\}_{l=1}^N$ such that the synthesized waveform $\sum_{l=1}^N \sum_{i=1}^{L_p} \hat{c}_i^l w^l(t - \hat{\tau}_i^l)$ is well matched to the received waveform $r(t)$.

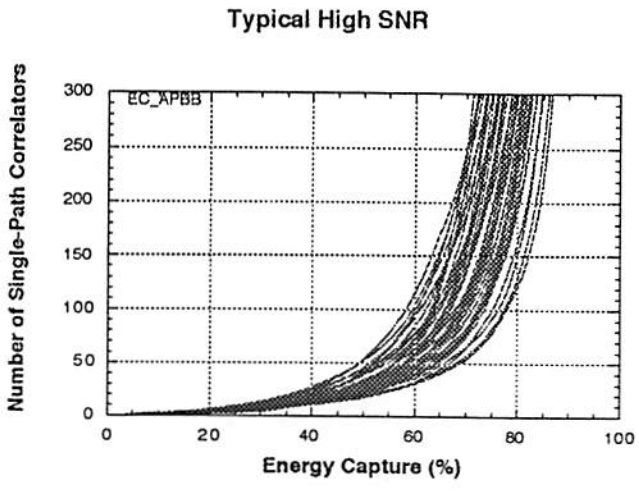

Fig. 5. The number of single-path signal correlators in a UWB Rake receiver as a function of percentage energy capture for each of the 49 received waveforms in an office representing typical "high SNR" environment.

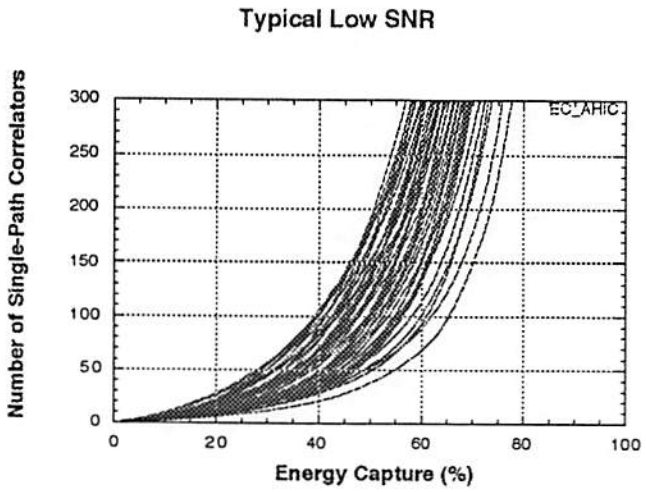

Fig. 6. The number of single-path signal correlators in a UWB Rake receiver as a function of percentage energy capture for each of the 49 received waveforms in an office representing typical "low SNR" environment.

ACKNOWLEDGMENTS

The authors wish to thank Mark A. Barnes, Alan Petroff and Larry Fullerton of Time Domain Systems, and Paul Withington of Pulson Communications for several helpful discussions concerning the technology, capabilities, and signal processing of impulse signals.

REFERENCES

[1] J. B. Andersen, T. S. Rappaport, and S. Yoshida, "Propagation measurements and models for wireless communications channels," *IEEE Commun. Mag.*, vol. 33, pp. 42–49, Jan. 1995.

[2] T. S. Rappaport and C. D. McGillem, "UHF fading in factories," *IEEE J. Select. Areas Commun.*, vol. SAC-7, pp. 40–48, Jan. 1989.

[3] T. S. Rappaport, "Characterization of UHF multipath radio channels in factory buildings," *IEEE Trans. Antennas Propagat.*, vol. AP-37, pp. 1058–1069, Aug. 1989.

[4] T. S. Rappaport, S. Y. Seidel, and K. Takamizawa, "Statistical channel impulse response models for factory an open plan building radio communication system design," *IEEE Trans. Commun.*, vol. COM-39, pp. 794–807, May 1991.

[5] S. Y. Seidel and T. S. Rappaport, "914 MHz path loss prediction models for indoor wireless communications in multifloored buildings," *IEEE Trans. Antennas Propagat.*, vol. AP-40, pp. 207–217, Feb. 1992.

[6] D. M. J. Devasirvatham, "Multipath time delay jitter measured at 850 MHz in the portable radio environment," *IEEE J. Select. Areas Commun.*, vol. SAC-5, pp. 855–861, June 1987.

[7] A. A. Saleh and R. A. Valenzuela, "A statistical model for indoor multipath propagation," *IEEE J. Select. Areas Commun.*, vol. SAC-5, pp. 128–137, Feb. 1987.

[8] R. J. Bultitude, S. A. Mahmoud, and W. A. Sullivan, "A comparison of indoor radio propagation characteristics at 910 MHz and 1.75 GHz," *IEEE J. Select. Areas Commun.*, vol. SAC-7, pp. 20–30, Jan. 1989.

[9] H. Hashemi, "The indoor radio propagation channel," *Proc. IEEE*, vol. 81, pp. 943–968, July 1993.

[10] G. Turin, F. D. Clapp, T. L. Johnston, S. B. Fine, and D. Lavry, "A statistical model of urban multipath propagation," *IEEE Trans. on Vehicul. Technol.*, vol. VT-21, pp. 1–9, Feb. 1972.

[11] G. Turin, "Introduction to spread-spectrum antimultipath techniques and their application to urban digital radio," *Proc. IEEE*, vol. 68, pp. 328–353, Mar. 1980.

[12] H. Suzuki, "A statistical model for urban radio propagation," *IEEE Trans. Commun.*, vol. 25, pp. 673–680, July 1977.

[13] H. Hashemi, "Simulation of the urban radio propagation channel," *IEEE Trans. on Vehicul. Technol.*, vol. VT-28, pp. 213–225, Aug. 1979.

[14] D. C. Cox, "Delay doppler characteristics of multipath propagation at 910 MHz in a suburban mobile radio environment," *IEEE Trans. Antennas Propagat.*, vol. AP-20, pp. 625–635, Sept. 1972.

[15] D. C. Cox, "Time- and frequency-domain characterizations of multipath propagation at 910 MHz in a suburban mobile-radio environment," *Radio Science*, pp. 1069–1077, Dec. 1972.

[16] D. C. Cox, "910 MHz urban mobile radio propagation: Multipath characteristics in New York city," *IEEE Trans. Commun.*, vol. COM-21, pp. 1188–1194, Nov. 1973.

[17] D. C. Cox and R. P. Leck, "Distributions of multipath delay spread and average excess delay for 910-MHz urban mobile radio paths," *IEEE Trans. Antennas Propagat.*, vol. AP-23, pp. 206–213, Mar. 1975.

[18] D. L. Nielson, "Microwave propagation measurements for mobile digital radio application," *IEEE Trans. on Vehicul. Technol.*, vol. VT-28, pp. 117–132, Aug. 1978.

[19] M. Z. Win, R. A. Scholtz, and M. A. Barnes, "Ultra-wide bandwidth signal propagation for indoor wireless communications," in *Proc. IEEE Int. Conf. on Comm.*, pp. 56–60, June 1997. Montréal, Canada.

[20] R. Price and P. E. Green, Jr., "A communication technique for multipath channels," *Proc. IRE*, vol. 46, pp. 555–570, Mar. 1958.

[21] J. G. Proakis, *Digital Communications*. McGraw-Hill, Inc., third ed., 1995.

[22] M. Z. Win and R. A. Scholtz, "Characterization of ultra-wide bandwidth wireless indoor communications channel: A communications theoretic view," *IEEE Trans. Commun.*, Nov. 1997. submitted.